Effects of echinacoside on the regulation of mitochondrial fission induced by TBK1/Drp1 in rheumatoid arthritis

Xiaoyan Wang^{1,A–F}, Zhufeng Chen^{2,B,C,F}, Shanshan Wu^{3,4,B,C,F}, Xuemei Fan^{5,A–C,E,F}

- ¹ Department of Diagnostics, Shaanxi University of Chinese Medicine, Xianyang, China
- ² Department of Orthopedics, Tangdu Hospital, The Second Affiliated Hospital of Air Force Medical University, Xi'an, China
- ³ Department of Anatomy, Basic Medical College, Shaanxi University of Chinese Medicine, Xianyang, China
- ⁴ Shaanxi Key Laboratory of Research on Traditional Chinese Medicine Physical Constitution and Treatment, Xianyang, China
- ⁵ Department of Rheumatology, Zibo Central Hospital, China
- A research concept and design; B collection and/or assembly of data; C data analysis and interpretation;
- D writing the article; E critical revision of the article; F final approval of the article

Advances in Clinical and Experimental Medicine, ISSN 1899-5276 (print), ISSN 2451-2680 (online)

Adv Clin Exp Med. 2025;34(11):1897-1906

Address for correspondence

Xuemei Fan

E-mail: xuemeifan198@163.com

Funding sources

This work was supported by the Natural Science Basic Research Program of Shaanxi Province (grant No. 2023-JC-QN-0852 and 2024JC-YBQN-0947), the project of Qinchuangyuan Traditional Chinese Medicine industry innovation cluster (grant No. L2024-QYC-ZYYJJQ-X15) and the Shaanxi Key Laboratory of Research on TCM Physical Constitution and Treatment (grant No. KF202308). The funders had no role in the study design, data collection and analysis, decision to publish, or preparation of the manuscript.

Conflict of interest

None declared

Acknowledgements

We thank Medjaden Inc. for providing scientific editing services for this manuscript.

Received on November 6, 2024 Reviewed on December 29, 2024 Accepted on January 8, 2025

Published online on July 2, 2025

Cite as

Wang X, Chen Z, Wu S, Fan X. Effects of echinacoside on the regulation of mitochondrial fission induced by TBK1/Drp1 in rheumatoid arthritis.

Adv Clin Exp Med. 2025;34(11):1897—1906.

doi:10.17219/acem/199920

DOI

10.17219/acem/199920

Copyright

Copyright by Author(s)
This is an article distributed under the terms of the
Creative Commons Attribution 3.0 Unported (CC BY 3.0)
(https://creativecommons.org/licenses/by/3.0/)

Abstract

Background. Dysregulated mitochondrial fission in synovial tissue is a key contributor to the progression of rheumatoid arthritis (RA), and echinacoside (ECH) has been shown to modulate this process in a mouse model of RA.

Objectives. This study aimed to investigate the effects of echinacoside (ECH) on the proliferation and inflammatory response of human fibroblast-like synoviocytes (MH7A cells), and to elucidate the potential underlying mechanisms.

Materials and methods. The expression and co-localization of TANK-binding kinase 1 (TBK1) and phosphorylated dynamin-related protein 1 (p-Drp1) in synovial tissues from patients with and without RA were analyzed. MH7A cells were exposed to either ECH or 0.1% dimethyl sulfoxide (DMSO). Cell proliferation was detected using Cell Counting Kit-8 (CCK-8) assay and reactive oxygen species (ROS) expression was detected with dichlorofluorescin (DCFH) staining. The levels of interleukin (IL)-6, IL-8, tumor necrosis factor alpha (TNF-α), cyclooxygenase (COX)-2, IL-1β, TANK-binding kinase 1 (TBK1), and Drp1 and the oxidative stress markers NF-E2-related factor 2 (Nrf2), heme oxygenase-1 (HO-1) and NAD(P)H: quinone oxidoreductase 1 (NQ01) were measured using quantitative real-time polymerase chain reaction (qPCR). The mitochondrial morphology was detected with transmission electron microscopy (TEM), and the expression levels of p-TBK1 (S172), TBK1, p-Drp1 (S616), p-Drp1 (S637), and Drp1 were assessed using western blotting.

Results. Compared to tissue from non-RA patients, RA synovial tissue exhibited higher expression and colocalization of TBK1 and phosphorylated Drp1 (p-Drp1). Following ECH treatment, MH7A cell proliferation and inflammatory cytokine secretion were reduced, while the expression of antioxidant stress markers was significantly increased. Furthermore, ECH treatment led to reduced levels of ROS, mitochondrial fragmentation and dysregulated mitochondrial fission in MH7A cells, along with decreased expression of p-TBK1 (Ser172) and p-Drp1 (Ser616), while p-Drp1 (Ser637) levels were increased.

Conclusions. Echinacoside regulates abnormal mitochondrial fission via the TBK1/Drp1 pathway, reducing the proliferation and inflammatory response of MH7A cells.

Key words: rheumatoid arthritis, mitochondrial fission, echinacoside

Highlight

- TBK1 is highly expressed in rheumatoid arthritis (RA) synovial tissue and may promote inflammation through Drp1-mediated mitochondrial fission.
- Echinacoside reduces inflammation and oxidative stress in RA-derived MH7A synoviocytes, highlighting its potential as a natural anti-inflammatory compound.
- Echinacoside alleviates mitochondrial dysfunction by inhibiting mitochondrial fission in MH7A cells.
- The anti-inflammatory effects of echinacoside in rheumatoid arthritis are linked to its regulation of the TBK1/Drp1 signaling pathway.

Background

Rheumatoid arthritis (RA) is a profoundly disabling disorder that predominantly impacts the joints, with an estimated prevalence of around 0.25–1% within the global population. In China, the prevalence of RA is about 0.42% and the disability rate is as high as 61.3%. At present, drug treatment for this condition achieves primarily symptomatic remission; the progression of RA is difficult to curb, posing a clinical challenge.

Dysregulated mitochondrial fission assumes a crucial role in the progression of numerous diseases.^{3,4} Our research group found abnormal mitochondrial fission in synovial tissue and fibroblast-like synoviocytes (FLSs) in patients with RA.⁵ Dynamin-related protein 1 (Drp1), a key regulatory molecule, mediates abnormal mitochondrial fission in FLSs, induces synovial proliferation and inflammation, and aggravates the progression of RA.⁵ Its effect on the induction of such fission is influenced strongly by post-translational modifications, including phosphorylation, ubiquitination, Simulation of Urban Mobility (SUMO), and acetylation. Phosphorylation of Drp1 at Ser616 promotes mitochondrial fission, whereas phosphorylation at Ser637, Ser412 and Ser684 inhibits the fission process.^{4,6}

TANK-binding kinase 1 (TBK1) is a serine/threonine protein kinase that plays a critical role in the initiation and progression of various diseases, particularly cancer and inflammatory disorders, by mediating protein phosphorylation, and has emerged as a key focus of recent research.^{7,8} It belongs to the non-classical IkB kinase family and exhibits 64% homology with IκB kinase ε (IKKε, also referred to as IKKi). In recent years, accumulating evidence has indicated that TBK1 is closely associated with the development of various cancers, particularly lung, pancreatic and colorectal cancers. It is significantly upregulated in KRAS-mutant pancreatic ductal adenocarcinoma, and the receptor tyrosine kinase AXL activates it through a RAS-RalB-dependent mechanism, enhancing the epithelial-mesenchymal transition of pancreatic cancer cells, thereby increasing their aggressiveness and metastatic potential.8 The elimination of TBK1 can reduce the occurrence of immune tolerance, increasing the anti-tumor immunotherapeutic effect of PD1.7 Inhibitors targeting TBK1 can significantly improve the effect of tumor

immunotherapy.⁷ On the other hand, overactivation of TBK1 is closely linked to immune dysregulation and is a key contributor to the pathogenesis of autoimmune diseases, $^{9-11}$ suggesting that TBK1 may represent a promising therapeutic target for the treatment of RA. However, Hu et al. 12 found that the local expression of TBK1 is low in the joints of patients with osteoarthritis, and that the overexpression of TBK1 ameliorated tumor necrosis factor alpha (TNF- α)-induced apoptosis and mitochondrial dysfunction. In addition, TBK1 mediates Drp1-S637 phosphorylation to inhibit mitochondrial fission, induces mitochondrial autophagy, maintains mitochondrial homeostasis and alleviates local joint inflammation in patients with osteoarthritis. 12

Echinacoside (ECH) is a phenylethanol glycoside with multiple biological functions. In recent years, the amount of basic research on ECH has increased, with studies focusing on its neuroprotective, anti-tumor, anti-oxidative, anti-inflammatory, and other functions. $^{13-16}$ Echinacoside has been shown to provide neuroprotection by suppressing the α -synuclein/TLR2/NF- κ B/NLRP3 pathway in microglia within a Parkinson's disease model. 17 Echinacoside has been shown to alleviate osteoarthritis in mice through activation of the Nrf2/HO-1 signaling pathway. 18 Additionally, ECH modulates oxidative stress and reduces alcohol-induced liver injury by targeting Nrf2. 19 We previously found that ECH effectively attenuated the progression of arthritis in CIA mice. 20 However, the effect of ECH on MH7A synovial cells in RA is still not understood.

Objectives

In this study, we investigated the expression of TBK1 in RA synovium and the effect of ECH on RA (MH7A synovial) cells via the TBK1/Drp1 pathway.

Materials and methods

Reagents

A Cell Counting Kit-8 (CCK-8; AC0011S) was purchased from Xi'an AccuRef Scientific (Xi'an, China). The reactive

oxygen species (ROS) probe DCFH-DA (S0033S) was obtained from Beyotime Biotechnology (Shanghai, China). TBK1 antibody (#3504, 51872S), p-TBK1 (S172; #5433), p-Drp1 (S616; #4494, 3455S), and Drp1 antibody (#8570) were purchased from Cell Signaling Technology (CST; Danvers, USA). GAPDH (ab181602) and p-Drp1 (S637; ab193216) were provided by Abcam (Cambridge, UK). Horseradish peroxidase (HRP)-conjugated goat anti-rabbit IgG was purchased from ASPEN (AS1107; Wuhan, China). Dulbecco's modified Eagle's medium (DMEM; G4524), fetal bovine serum (FBS; G8002) and HRP-labeled goat anti-mouse IgG (GB23301) were obtained from Servicebio (Wuhan, China). A sodium dodecyl sulfate-polyacrylamide gel electrophoresis (SDS-PAGE) gel preparation kit (AS1012), a bicinchoninic acid (BCA) protein concentration determination kit (AS1086), radioimmunoprecipitation (RIPA) total protein lysate (AS1004), electrochemiluminescence (ECL) detection kit (AS1059), protease inhibitor cocktail (04693159001), and phosphorylase inhibitor (AS1008) were bought from ASPEN. A rapid RNA extraction kit (RM0051) was purchased from AccuRef Scientific. EntiLink™ 1st-strand cDNA synthesis super mix (EQ031), TRIpure total RNA extraction reagent, and EnTurbo™ SYBR Green PCR SuperMix (EQ001) were acquired from ELK Biotechnology (Wuhan, China). Primers were obtained from Sangong Biotech (Shanghai, China).

Study design

The MH7A cell line (No. CL-474h), an immortalized cell line derived from RA FLS transfected with SV40T antigen gene that has the characteristics of human RA-FLS, was utilized to analyze the impact of ECH on cell proliferation, inflammatory cytokine levels, oxidative stress, mitochondrial morphology, and mitochondrial phosphorylation.

Participants

Patients with RA who underwent knee replacement surgery (n = 6) and those with meniscus injury but not RA who underwent arthroscopic surgery (n = 4) were incorporated into this study. The research recerived approval from the Institutional Review Board of Tangdu Hospital, Air Force Medical University, Xi'an, China (approval No. TDLL-202408-08).

Cell source and culture

MH7A cells (cell line No. CL-474h) were purchased from SAIOS (Wuhan, China). They were removed from storage in liquid nitrogen, immediately placed in a water bath set at 37.5°C, shaken for rapid recovery, and quickly moved to a super-clean table. Each cell sample was moved into a 15-mL centrifuge tube, where 2 mL of DMEM (supplemented with 10% FBS and 1% penicillin–streptomycin solution) was added before centrifuging at 1,000 rpm for 5 min. After discarding the supernatant, 10 mL of medium was added for

resuspension, and each sample was then inoculated in a culture bottle and placed in a cell incubator for culture. The medium was changed daily. When the cells reached >80% confluence, as confirmed using optical microscopy (Zeiss Primovert Hdcam; Carl Zeiss AG, Oberkochen, Germany) the trypsin was digested and cultured. Cells in the logarithmic phase of growth were randomly assigned to either the dimethyl sulfoxide (DMSO) group or the ECH group.

Immunofluorescence and co-localization analysis

The synovial tissues were preserved overnight in 10% formalin and subsequently embedded in paraffin. Paraffin sections were dewaxed and hydrated, and antigen repair and hydrogen peroxide and serum sealing were performed. Primary antibodies (TBK1 and p-DRP1 S616, 1:1,000) were added and the samples were left to rest overnight at 4°C. Then, the secondary antibody (1:500) was applied, and the samples were left to incubate for 50 min. The Tyramide Signal Amplification (TSA) was then added, and the samples were kept at room temperature for an additional 10 min. Following microwave treatment, the primary and secondary antibodies were removed, and the samples were incubated with 10% rabbit serum (cat. No. G1209) or 3% BSA at room temperature for 30 min to block nonspecific binding. Subsequently, DAPI (4',6-diamidino-2-phenylindole) was added to re-stain the nuclei, and the samples were incubated at room temperature for 10 min in the dark. The samples were then washed 3 times with PBS for 5 min each, after which a fluorescence quencher was applied. The tissue slices were loaded into a PAN-NORAMIC digital slide scanner (3DHISTECH, Budapest, Hungary) for imaging. All tissue imaging information was uploaded into a folder and viewed (at $\times 1$ –400 magnification) using CaseViewer v. 2.4 software (3DHISTECH). The Area Quantification FL module v. 2.1.2 (Indica Labs, Albuquerque, USA) was used with the Halo analytical software v. 3.0.311.314 (Indica Labs) to quantify the numbers of gene-positive cells and positive and tissue areas in each section, the positive cell density (number of positive cells/tissue area), and the percentage of positive area (positive area/tissue area × 100%).

Transmission electron microscopy

Six-well plates were inoculated with 1×10^6 cells each. The DMSO group was treated with 0.1% DMSO solution and the ECH group was treated with ECH (100 µmol/L) for 24 h, with or without interleukin (IL)-1 β (10 ng/mL) for 30 min. About 1 mL of electron microscopy fixative was added to the cells for 2 h before being stored at 4°C. They were washed 3 times with 0.1 M phosphate buffer (PB; pH 7.4) for 15 min. After fixation, dehydration, permeabilization, embedding, and sectioning, the cells were double-stained with 2% uranyl acetate and lead citrate for 15 min each, then left to dry overnight at room temperature. Samples were examined using transmission electron

microscopy (TEM; HT7700; Hitachi High Technologies, Tokyo, Japan) and super-resolution microscopy, and images were collected for further analysis.

CCK-8 assay

Ninety-six-well plates were inoculated with 1×10^5 cells each, and each group was set with 6 compound pores. The samples were treated with DMSO (0.1%) or ECH (40, 80 and 100 μM). Twenty-four hours later, 10 μL of CCK-8 reagent was added for 2 h. Absorbance (OD450) was detected using a microplate reader (Infinite F50; Tecan, Männedorf, Switzerland)

qPCR

Six-well plates were inoculated with 1×10^6 cells each. The samples were treated with 0.1% DMSO solution or $100~\mu mol/L$ ECH for 24~h. Total RNA was isolated using a rapid RNA extraction kit, and its purity and concentration were detected with ultraviolet spectrophotometry. The RNA underwent reverse transcription to cDNA utilizing the EntiLinkTM 1st-strand cDNA synthesis super mix kit and was subsequently stored at -20° C. Following this, quantitative real-time polymerase chain reaction (qPCR) was conducted with the EnTurboTM SYBR Green PCR SuperMix kit, employing a $10-\mu$ L reaction system. The CT values were determined based on the $2^{-\Delta\Delta CT}$ method. The primers used are detailed in Table 1.

Western blotting

Six-well plates were inoculated with 1×10^6 cells each. The samples were exposed to 0.1% DMSO solution or 100 μ mol/L ECH for 24 h, with or without IL-1 β (10 ng/ mL) for 30 min. The protein extraction process was carried out using a RIPA lysate that contained a protease and phosphatase inhibitor. The BCA quantification was performed according to the kit (P0010S; Beyotime) instructions. Briefly, a standard curve was made and sample protein concentrations were determined. Protein denaturation, SDS-PAGE electrophoresis, membrane transfer and closure, primary antibody incubation (p-Drp1 (S616), 1:500; p-Drp1 (S637), 1:500; Drp1, 1:2,000; p-TBK1 (S172), 1:1,000; TBK1, 1:3,000; GAPDH, 1:10,000), secondary antibody incubation (1:10,000), and development were performed. A chemiluminescence imaging analysis system was used for image collection and an AlphaEaseFC software processing system (Alpha Innotech, San Leandro, USA) was employed to assess the optical densities (ODs) of the specific bands.

ROS DCFH-DA staining

The levels of ROS in the cells were evaluated using dichlorofluorescin (DCFH) staining. Following a 24-h

Table 1. Primer sequences

Gene	Туре	Sequence
H-GAPDH	sense	CATCATCCCTGCCTCTACTGG
	antisense	GTGGGTGTCGCTGTTGAAGTC
H-IL-6	sense	TCAGCCCTGAGAAAGGAGACAT
	antisense	GCTCTGGCTTGTTCCTCACTACT
H-IL-8	sense	ACTGAGAGTGATTGAGAGTGGAC
	antisense	AACCCTCTGCACCCAGTTTTC
H-TNF-a	sense	CTCTTCTCCTTCCTGATCGTGG
	antisense	CTTGTCACTCGGGGTTCGAG
H-COX-2	sense	AGATTATGTGCAACACTTGAGTGG
	antisense	ATTCCTACCACCAGCAACCCT
H-IL-1β	sense	ACGATGCACCTGTACGATCACT
	antisense	GAGAACACCACTTGTTGCTCCA
H-TBK1	sense	TATTTGCTATTGAAGAGGAGACAAC
	antisense	TAGTCCATAGGCATTAGAAGGTTCT
H-Drp1	sense	ATTCCATTATCCTCGCTGTCACT
	antisense	TGGCTCCTGTTAACTACTCCAAT
H-NQO1	sense	TGGTGGAGTCGGACCTCTATG
	antisense	CATGGCAGCGTAAGTGTAAGC
H-HO-1	sense	GCCAGCAACAAGTGCAAGA
	antisense	TAAGGACCCATCGGAGAAGC
H-Nrf2	sense	GACAGCCCTGGTATTGATGTC
	antisense	TCACCTTGTGGAAGAAGTGCTT

treatment with either DMSO or ECH, the medium was discarded and DCFH (10 $\mu M)$ was introduced. The samples were incubated at 37°C for 30 min in the dark, then rinsed 3 times with fresh cell medium for 5 min each time. Hoechst nucleic acid stain was applied, and the samples were kept at room temperature away from light for an additional 5 min. Subsequently, the samples were washed 3 additional times with fresh medium for 5 min each, then examined under a fluorescence microscope, and images were captured for analysis.

Statistical analyses

Statistical analysis was conducted using IBM SPSS v. 19.0 (IBM Corp., Armonk, USA). The Shapiro–Wilk test assessed the normality of the data, while the Levene's statistic evaluated homogeneity of variance. For normally distributed data with equal variances, an independent-samples t-test was used for comparisons between 2 groups, while one-way analysis of variance (ANOVA) was applied for comparisons among three groups. Post hoc comparisons were conducted using the Student–Newman–Keuls (SNK) test. Non-normally distributed data were analyzed with the Wilcoxon rank sum test. P-values less than 0.05 were considered statistically significant.

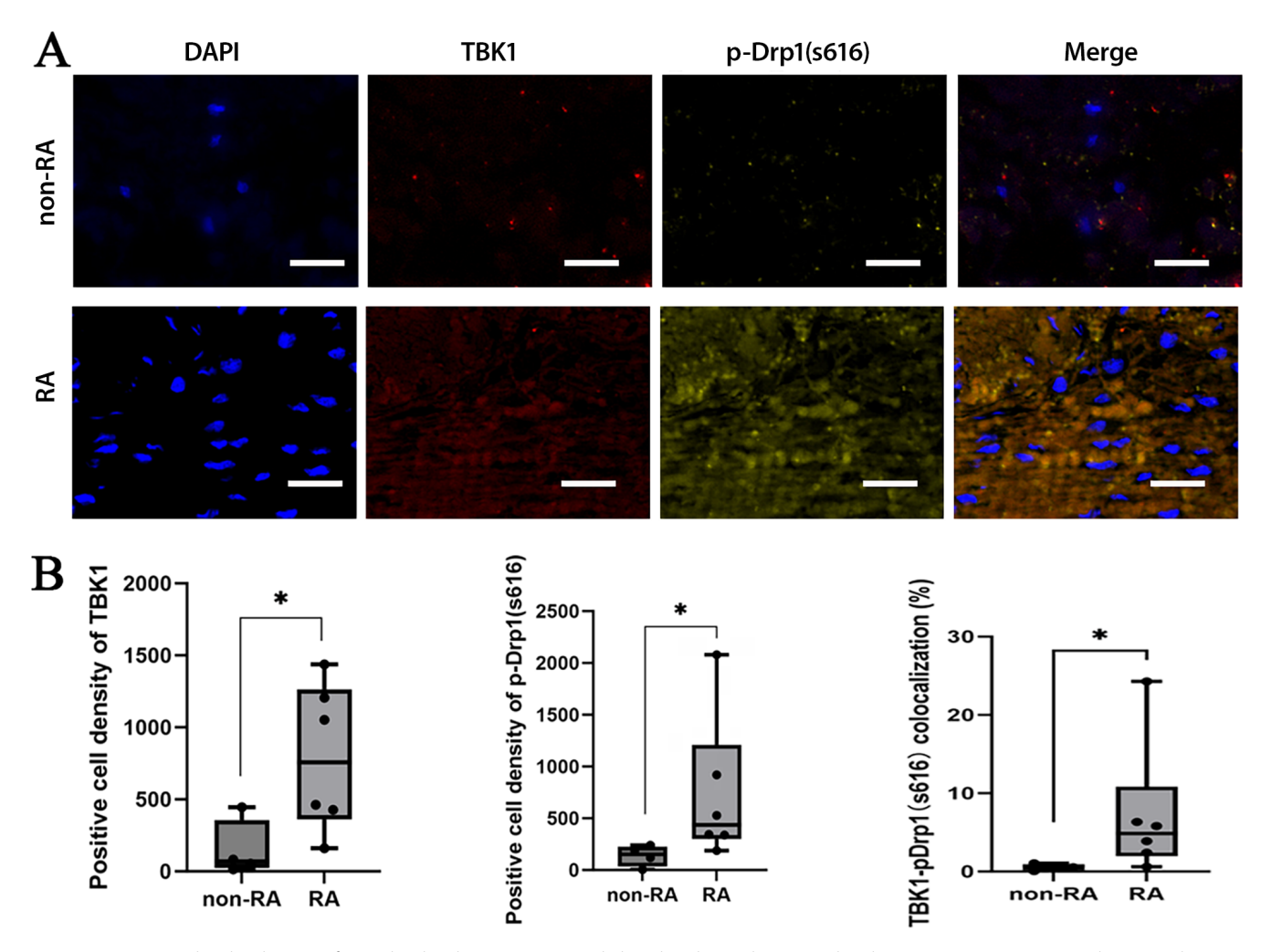


Fig. 1. Expression and co-localization of TANK-binding kinase 1 (TBK1) and phosphorylation dynamin-related protein 1 (p-Drp1) (S616) in rheumatoid arthritis (RA) synovial tissue. A. Expression and co-localization of TBK1 and p-Drp1 (S616) in the synovial tissue of patients with (n = 6) and without (n = 4) RA, detected using immunofluorescence staining (scale: $20 \mu m$); B. Densities and co-localization of TBK1- and p-Drp1 (S616)-positive cells in the synovial tissue of patients with and without RA

*p < 0.05, Wilcoxon rank sum test.

Results

Expression and co-localization of TBK1 and p-Drp1 (S616) in RA synovial tissue

Overactivation of TBK1 is closely associated with dysregulation of the immune response and plays a key role in the pathogenesis of autoimmune diseases. To investigate whether TBK1 is upregulated and involved in Drp1-mediated mitochondrial fission in rheumatoid arthritis (RA), we analyzed the expression and co-localization of TBK1 and phosphorylated Drp1 (p-Drp1) in RA synovial tissues. The expression of TBK1, p-Drp1 (S616) and their co-localization in synovial tissue were higher in the RA group compared to the non-RA group (Fig. 1). This high expression of TBK1 in RA synovium may be related to Drp1-mediated mitochondrial fission.

Effects of ECH on MH7A cell proliferation and inflammation

Previous studies demonstrated that ECH effectively attenuates arthritis progression in collagen-induced arthritis (CIA) mice. Here, we investigate the effects of ECH on MH7A cell proliferation and inflammation. The proliferation of MH7A cells declined after ECH treatment (Fig. 2A). The qPCR analysis revealed that treatment with 100 μ mol/L ECH significantly increased the mRNA expression of antioxidant stress markers HO-1, NQO1 and Nrf2 (Fig. 2B), while reducing the expression of inflammatory cytokines IL-6, IL-8, TNF- α , COX-2, and IL-1 β (Fig. 2C). These results suggest that ECH alleviated MH7A cell inflammation and oxidative stress.

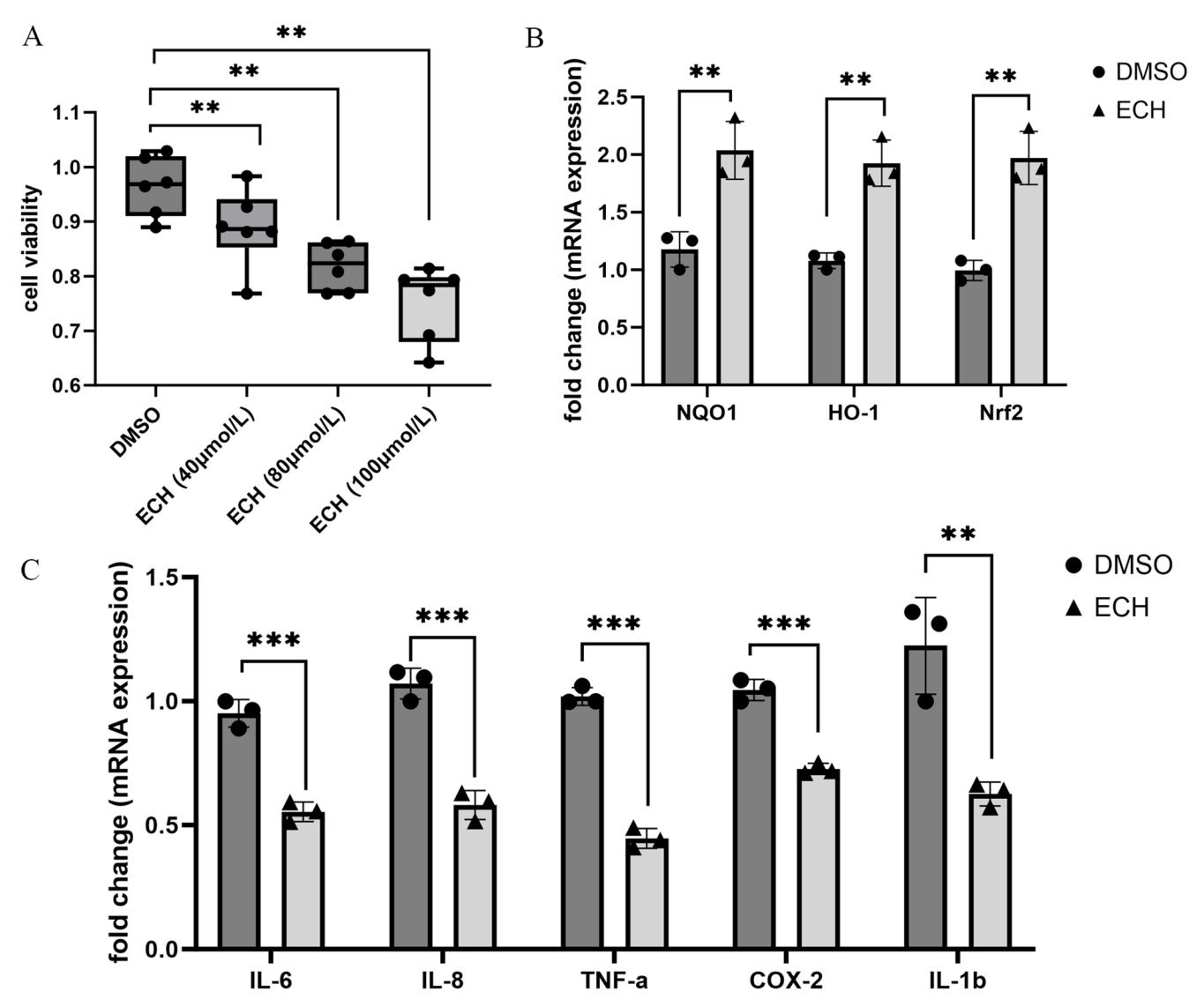


Fig. 2. Effects of echinacoside (ECH) treatment on MH7A cell proliferation and inflammation. A. Cell proliferation activity detected using Cell Counting Kit-8 (CCK-8) assay and assessed with analysis of variance (ANOVA); B. Expression of heme oxygenase-1 (HO-1), NAD(P)H: quinone oxidoreductase 1 (NQO1) and NF-E2-related factor 2 (Nrf2), , detected with quantitative real-time polymerase chain reaction (qPCR). Data are presented as mean \pm standard deviation (SD); C. Expression of the inflammatory cytokines interleukin (IL)-6, IL-8, tumor necrosis factor alpha (TNF-q), cyclooxygenase-2 (COX-2), and IL-1 β , detected with qRT-PCR

Effects of ECH on oxidative stress and mitochondrial fission of MH7A cells

Mitochondrial fission is involved in synovium inflammation, as it induces oxidative stress. To clarify the effect of ECH on mitochondrial fission, ROS expression and mitochondrial morphology were examined. After ECH treatment, ROS expression was significantly decreased in MH7A cells (Fig. 3A). Transmission electron microscopy revealed that IL-1 β induced mitochondrial fission in the cells, but that this fission was significantly reduced after ECH treatment (Fig. 3B). No significant differences were observed in the mRNA expression levels of TBK1 and Drp1 between the treatment and control groups (Fig. 3C). These findings suggest that ECH alleviates inflammation and oxidative stress in MH7A cells by inhibiting mitochondrial fission.

Effects of ECH on TBK1 and Drp1 expression in MH7A cells

Next, we investigated the effects of ECH on the expression levels of TBK1, phosphorylated TBK1 (p-TBK1), Drp1, and phosphorylated Drp1 (p-Drp1). Western blot analysis showed that IL-1 β stimulation increased the level of phosphorylated TBK1 at Ser172 (p-TBK1^S172), which was subsequently reduced following ECH treatment (Fig. 4A,B). In addition, IL-1 β induced upregulation of phosphorylated Drp1 at Ser616 (p-Drp1^S616) and downregulation at Ser637 (p-Drp1^S637), effects that were reversed by ECH treatment (Fig. 4C,D). These findings suggest that ECH inhibits mitochondrial fission in MH7A cells by regulating the TBK1/Drp1 pathway.

^{**}p < 0.01, ***p < 0.001.

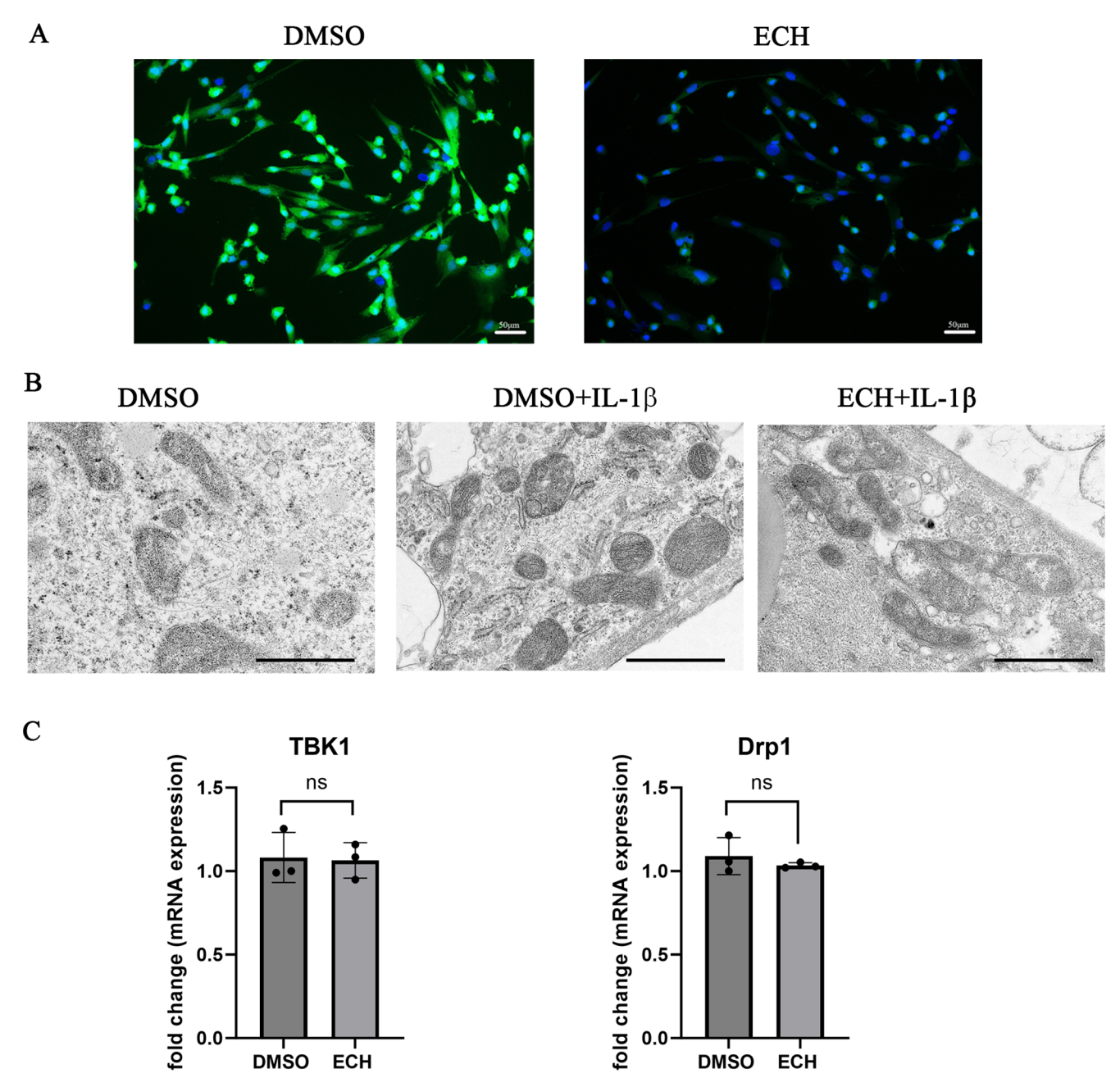


Fig. 3. Effects of echinacoside (ECH) on oxidative stress and mitochondrial fission of MH7A cells. A. Reactive oxygen species (ROS) expression detected using dichlorofluorescein (DCFH) staining (scale: 50 μm); B. Mitochondrial morphology detected with transmission electron microscopy (TEM; scale: 1 μm); C. dynamin-related protein 1 (Drp1) and TANK-binding kinase 1 (TBK1) expression detected with quantitative real-time polymerase chain reaction (qPCR). The data are presented as mean ± standard deviation (SD)

ns - nonsignificant; p > 0.05.

Discussion

This study demonstrated that TBK1 expression was markedly elevated in the synovial tissue of RA patients, consistent with findings from animal models of RA, but in contrast to the lower expression levels observed in the synovial tissue of patients with OA.¹² Our results provide further support for TBK1 as a potential therapeutic target for RA.

A 2023 report indicated that local TBK1 expression is low in the joints of patients with OA. ¹² In contrast, a 2022 study

using a rat model of RA reported elevated levels of phosphorylated TBK1 (p-TBK1). In that study, treatment with CS12192, a novel small-molecule inhibitor selectively targeting JAK3, JAK1, and TBK1, and WEHI112 – a relatively selective TBK1 inhibitor, produced notable immunosuppressive and anti-inflammatory effects. ¹⁰ Similar to this report, our findings showed that the expression of TBK1 was upregulated in RA synovial tissues. According to a 2021 report, ²¹ TBK1 also plays a critical role in the activation of innate immunity by regulating RIPK1-dependent cell death

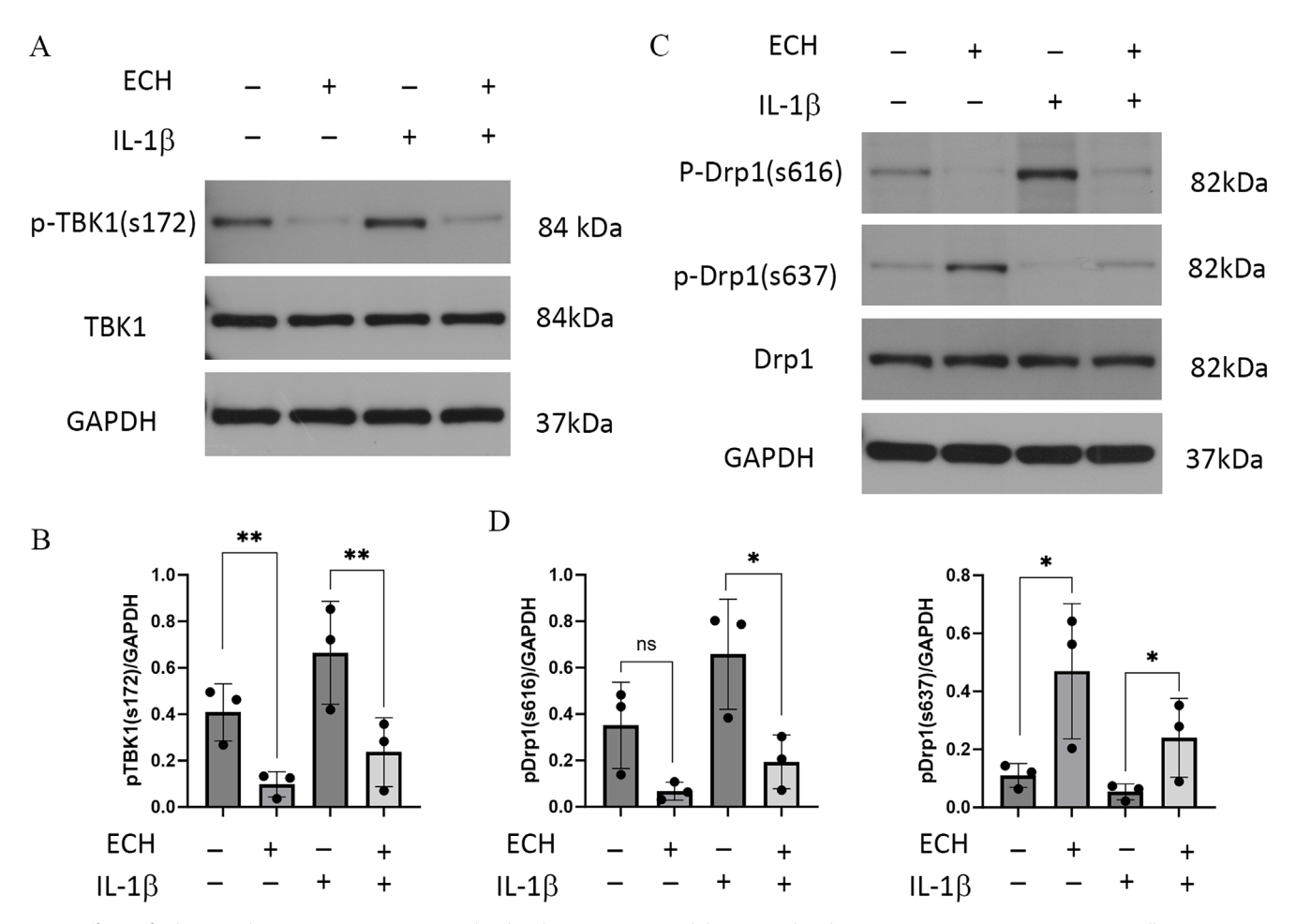


Fig. 4. Effects of echinacoside (ECH) treatment on TANK-binding kinase 1 (TBK1) and dynamin-related protein 1 (Drp1) expression in MH7A cells. A,B. p-TBK1 (s172) and TBK1 expression levels detected with western blotting; C,D. p-Drp1 (S616), p-Drp1 (S637) and Drp1 expression levels detected with western blotting. The concentration of ECH was 100 μ mol/L and the concentration of interleukin (IL)-1 β was 10 ng/mL. The data are presented as mean \pm standard deviation (SD)

ns – nonsignificant; p > 0.05; *p < 0.05; **p < 0.01.

pathways triggered by type I interferons (IFN-I), NF-κB (nuclear factor kappa-light-chain-enhancer of activated B cells) and TNF. In 4 patients with congenital immunodeficiency, a biallelic loss-of-function (LoF) mutation in the TBK1 gene was identified, which resulted in excessive TNF-induced cell death and subsequent autoimmune inflammation. Notably, treatment with anti-TNF therapy effectively mitigated these pathological effects. 21 These findings further demonstrate the different roles of TBK1 in autoimmune diseases, which may be related to the post-translational modification of TBK1. According to a 2020 report, TBK1 and Drp1 are vital for congenital RNA sensing and antiviral immunity, and TBK1-mediated Drp1 phosphorylation at S412 and S684 affects mitochondrial fission, enhancing the host antiviral defense.²² In this study, we observed increased colocalization of TBK1 and p-Drp1 (Ser616) in the synovial tissue of patients with RA, suggesting that TBK1 may mediate the activation of p-Drp1 (Ser616), thereby contributing to Drp1-dependent mitochondrial fission in this tissue.

Excessive ROS accumulation is a key factor in the oxidative stress response of FLSs. According to a 2020

report, ROS overexpression in FLSs triggers the secretion of inflammatory mediators, including IL-6 and IL-8, via the NF-κB signaling pathway.²³ In this study, we evaluated the effects of various concentrations of ECH on ROS expression in MH7A cells and found that only 100 µmol/L ECH significantly reduced ROS levels, whereas other concentrations showed no notable effect (data not shown). Therefore, 100 µmol/L ECH was selected as the working concentration for subsequent experiments. Echinacoside effectively reduced the mRNA expression of inflammatory cytokines in MH7A cells, while simultaneously upregulating the expression of antioxidant stress markers, including Nrf2, HO-1 and NQO1. These findings suggest that ECH may alleviated MH7A cell inflammation and oxidative stress. Several studies have reported that ECH effectively modulates the oxidative stress response. A 2019 study reported that ECH significantly reduces ROS and NF-κB levels by inhibiting the NLRP3 inflammasome signaling pathway in spinal cord injury models.²⁴ Similarly, a 2022 study demonstrated that ECH prevents pyroptosis in cardiomyocytes and improves cardiac function by modulating the NADPH/ROS/endoplasmic reticulum (ER) stress pathways. ²⁵ Consistent with previous findings, ^{18,26} these results support the notion that ECH exerts therapeutic effects through its antioxidant properties.

In addition, as reported in 2020, ECH significantly inhibits Drp1, reverses abnormal mitochondrial fission at lesion sites, protects mitochondrial function and inhibits ROS-mediated oxidative stress, thereby reducing neuroinflammation.²⁷ The anti-oxidative stress effect of ECH may be closely related to the regulation of mitochondrial fission. Consistent with these findings, our team reported in 2024 that ECH reversed abnormal mitochondrial fission in the joints of CIA mice, thereby alleviating arthritic manifestations, by inhibiting Drp1.20 In this study, we further found that ECH effectively reversed abnormal mitochondrial fission in MH7A cells, strengthening the conclusion that ECH alleviates inflammation and oxidative stress in these cells by inhibiting mitochondrial fission. However, ECH had no effect on Drp1 or TBK1 mRNA expression. The phosphorylated forms of these proteins play important roles in cell signaling, and ECH may regulate their phosphorylation. In this study, ECH notably decreased the levels of p-TBK1 (S172) and p-Drp1 (S616), while simultaneously enhancing the expression of p-Drp1 (S637). We believe that ECH inhibits mitochondrial fission in synovial tissue through the activation of TBK1 to mediate p-Drp1 (S616) phosphorylation and inhibit the proliferation and inflammation and oxidative stress induction of MH7A cells. In contrast to our findings, a 2023 study reported that TBK1 inhibits mitochondrial fission by promoting the phosphorylation of Drp1 at Ser637, thereby inducing mitophagy, maintaining mitochondrial homeostasis and alleviating local joint inflammation. 12 These findings suggest that the mitochondrial functions of TBK1 may differ between the synovial tissue of patients with OA and RA. In RA, TBK1 may contribute to disease progression by promoting mitochondrial fission through the phosphorylation of Drp1 at Ser616. This hypothesis warrants further investigation in future studies.

Limitations

This study has several limitations. First, the safety profile of ECH was not assessed and warrants further investigation. Second, we did not determine whether ECH modulates Drp1 phosphorylation in a TBK1-dependent manner, which remains to be elucidated. Finally, the TBK1-knockout mouse model used in this study requires further refinement to better clarify the mechanistic role of TBK1 in vivo.

Conclusions

The results of this study suggest that ECH treatment inhibits TBK1 phosphorylation, thereby modulating mitochondrial fission and p-Drp1 levels, ultimately leading

to reduced ROS production and inflammation in MH7A cells. Echinacoside may suppress abnormal mitochondrial fission in MH7A cells by modulating the TBK1/Drp1 signaling pathway, thereby inhibiting cell proliferation and the inflammatory response. These findings suggest that ECH could represent a promising novel therapeutic option for the treatment of RA.

Data availability statement

The datasets supporting the findings of the current study are openly available in Zenodo repository at https://doi.org/10.5281/zenodo.14783921.

Consent for publication

Not applicable.

Use of AI and AI-assisted technologies

Not applicable.

ORCID

References

- Di Matteo A, Bathon JM, Emery P. Rheumatoid arthritis. Lancet. 2023; 402(10416):2019–2033. doi:10.1016/S0140-6736(23)01525-8
- Geng Y, Xie X, Wang Y, et al. The standardized diagnosis and treatment of rheumatoid arthritis [in Chinese]. Zhonghua Nei Ke Za Zhi. 2022;61(1):51–59. doi:10.3760/cma.j.cn112138-20210616-00426
- Kleele T, Rey T, Winter J, et al. Distinct fission signatures predict mitochondrial degradation or biogenesis. *Nature*. 2021;593(7859):435–439. doi:10.1038/s41586-021-03510-6
- Chen W, Zhao H, Li Y. Mitochondrial dynamics in health and disease: mechanisms and potential targets. Sig Transduct Target Ther. 2023;8(1):333. doi:10.1038/s41392-023-01547-9
- Wang X, Chen Z, Fan X, et al. Inhibition of DNM1L and mitochondrial fission attenuates inflammatory response in fibroblast-like synoviocytes of rheumatoid arthritis. *J Cell Mol Med*. 2020;24(2):1516–1528. doi:10.1111/jcmm.14837
- Weyand CM, Wu B, Huang T, Hu Z, Goronzy JJ. Mitochondria as disease-relevant organelles in rheumatoid arthritis. Clin Exp Immunol. 2023;211(3):208–223. doi:10.1093/cei/uxac107
- Sun Y, Revach OY, Anderson S, et al. Targeting TBK1 to overcome resistance to cancer immunotherapy. *Nature*. 2023;615(7950):158–167. doi:10.1038/s41586-023-05704-6
- Xiang S, Song S, Tang H, et al. TANK-binding kinase 1 (TBK1): An emerging therapeutic target for drug discovery. *Drug Discovery Today*. 2021;26(10):2445–2455. doi:10.1016/j.drudis.2021.05.016
- Louis C, Ngo D, D'Silva DB, et al. Therapeutic effects of a TANK-binding kinase 1 inhibitor in germinal xenter-driven collagen-induced arthritis. Arthritis Rheum. 2019;71(1):50–62. doi:10.1002/art.40670
- Fang Z, Hu Y, Dai J, et al. CS12192, a novel JAK3/JAK1/TBK1 inhibitor, synergistically enhances the anti-inflammation effect of methotrexate in a rat model of rheumatoid arthritis. *Int J Mol Sci.* 2022; 23(21):13394. doi:10.3390/ijms232113394
- Zeng Y, Ng JPL, Wang L, et al. Mutant p53R211* ameliorates inflammatory arthritis in AIA rats via inhibition of TBK1-IRF3 innate immune response. *Inflamm Res.* 2023;72(12):2199–2219. doi:10.1007/s00011-023-01809-w

- Hu SL, Mamun AA, Shaw J, et al. TBK1-medicated DRP1 phosphorylation orchestrates mitochondrial dynamics and autophagy activation in osteoarthritis. Acta Pharmacol Sin. 2023;44(3):610–621. doi:10.1038/ s41401-022-00967-7
- Song Y, Zeng K, Jiang Y, Tu P. Cistanches Herba, from an endangered species to a big brand of Chinese medicine. Med Res Rev. 2021;41(3): 1539–1577. doi:10.1002/med.21768
- Chuang HW, Wang TY, Huang CC, Wei IH. Echinacoside exhibits antidepressant-like effects through AMPAR-Akt/ERK-mTOR pathway stimulation and BDNF expression in mice. *Chin Med*. 2022;17(1):9. doi:10.1186/s13020-021-00549-5
- Li W, Zhou J, Zhang Y, et al. Echinacoside exerts anti-tumor activity via the miR-503-3p/TGF-β1/Smad aixs in liver cancer. Cancer Cell Int. 2021;21(1):304. doi:10.1186/s12935-021-01890-3
- Ma Y, Yang X, Jiang N, Lu C, Zhang J, Zhuang S. Echinacoside ameliorates doxorubicin-induced cardiac injury by regulating GPX4 inhibition-induced ferroptosis. Exp Ther Med. 2023;27(1):29. doi:10.3892/etm.2023.12317
- Yang XP, Huang JH, Ye FL, et al. Echinacoside exerts neuroprotection via suppressing microglial α-synuclein/TLR2/NF-κB/NLRP3 axis in parkinsonian models. *Phytomedicine*. 2024;123:155230. doi:10.1016/j. phymed.2023.155230
- Tan Z, Zhang B. Echinacoside alleviates osteoarthritis in rats by activating the Nrf2-HO-1 signaling pathway. *Immunopharmacol Immunotoxicol*. 2022;44(6):850–859. doi:10.1080/08923973.2022.2088384
- Ding Y, Zhang Y, Wang Z, et al. Echinacoside from Cistanche tubulosa ameliorates alcohol-induced liver injury and oxidative stress by targeting Nrf2. FASEB J. 2023;37(3):e22792. doi:10.1096/fj.202201430R

- 20. Wang X, Li L, Zhang M, et al. Anti-inflammatory effect of echinacoside in collagen-induced arthritis via Nrf2/Drp1 pathway [published online as ahead of print on March 20, 2024]. *Adv Clin Exp Med*. 2024. doi:10.17219/acem/184640
- Taft J, Markson M, Legarda D, et al. Human TBK1 deficiency leads to autoinflammation driven by TNF-induced cell death. *Cell.* 2021; 184(17):4447–4463.e20. doi:10.1016/j.cell.2021.07.026
- Chen S, Liu S, Wang J, et al. TBK1-mediated DRP1 targeting confers nucleic acid sensing to reprogram mitochondrial dynamics and physiology. *Mol Cell*. 2020;80(5):810–827.e7. doi:10.1016/j.molcel. 2020 10 018
- Nygaard G, Firestein GS. Restoring synovial homeostasis in rheumatoid arthritis by targeting fibroblast-like synoviocytes. *Nat Rev Rheumatol*. 2020;16(6):316–333. doi:10.1038/s41584-020-0413-5
- 24. Gao S, Xu T, Guo H, et al. Ameliorative effects of echinacoside against spinal cord injury via inhibiting NLRP3 inflammasome signaling pathway. *Life Sci.* 2019;237:116978. doi:10.1016/j.lfs.2019.116978
- Ni Y, Zhang J, Zhu W, Duan Y, Bai H, Luan C. Echinacoside inhibited cardiomyocyte pyroptosis and improved heart function of HF rats induced by isoproterenol via suppressing NADPH/ROS/ER. *J Cell Mol Med*. 2022;26(21):5414–5425. doi:10.1111/jcmm.17564
- Tao Z, Zhang L, Wu T, Fang X, Zhao L. Echinacoside ameliorates alcohol-induced oxidative stress and hepatic steatosis by affecting SREB-P1c/FASN pathway via PPARa. Food Chem Toxicol. 2021;148:111956. doi:10.1016/j.fct.2020.111956
- Zhou L, Yao M, Tian Z, et al. Echinacoside attenuates inflammatory response in a rat model of cervical spondylotic myelopathy via inhibition of excessive mitochondrial fission. Free Radic Biol Med. 2020; 152:697–714. doi:10.1016/j.freeradbiomed.2020.01.014